

DMD#81083

11 β -Hydroxysteroid Dehydrogenase 1 Human Tissue Distribution, Selective Inhibitor and Role in Doxorubicin Metabolism

Xin Yang, Wenyi Hua, Sangwoo Ryu, Phillip Yates, Cheng Chang, Hui Zhang, Li Di

Pharmacokinetics, Dynamics and Metabolism, Pfizer Inc., Groton, CT 06340, USA (XY,
WH, SR, HZ, LD); Early Clinical Development, Pfizer Inc., Cambridge, MA 02139, USA
(PY); Clinical Pharmacology, Pfizer Inc., Groton, CT 06340, USA (CC)

DMD#81083

Running Title: 11 β -HSD1 Tissue Distribution and Doxorubicin Metabolism

Corresponding Authors:

Hui Zhang

Pharmacokinetics, Dynamics and Metabolism,

Pfizer Inc., Eastern Point Road, Groton, CT 06340

Hui.Zhang3@Pfizer.Com

Li Di

Pharmacokinetics, Dynamics and Metabolism,

Pfizer Inc., Eastern Point Road, Groton, CT 06340

Li.Di@Pfizer.Com

Text Pages: 24

Tables: 4

Figures: 5

References: 29

Abstract: 126

Introduction: 603

Discussion: 678

DMD#81083

Abbreviations

AKR, aldo-keto reductase; CBR1, carbonyl reductase 1; CO₂, carbon dioxide;
CYP, cytochrome P450; DMF, dimethylformamide; DMSO, dimethyl sulfoxide;
ER, endoplasmic reticulum; HHEP, human hepatocyte; HLM, human liver microsomes;
HPLC, high performance liquid chromatography; 11 β -HSD1, 11 β -hydroxysteroid
dehydrogenase 1; 11 β -HSD2, 11 β -hydroxysteroid dehydrogenase 2; hr-11 β -HSD1,
human recombinant 11 β -hydroxysteroid dehydrogenase 1; IDA, information-dependent
acquisition; IS, internal standard; LC, liquid chromatography; LC-MS/MS, liquid
chromatographic-tandem mass spectrometry; LOQ, lower limit of quantitation;
MS, mass spectrometry; NAD⁺, nicotinamide adenine dinucleotide; NADP⁺,
nicotinamide adenine dinucleotide phosphate; NNK, nicotine-derived nitrosamine ketone;
NADPH, nicotinamide adenine dinucleotide phosphate hydrogen; NNK, nicotine-derived
nitrosamine ketone; PBPK, physiological based pharmacokinetic; RAF, relative activity
factor; REF, relative expression factor; SRM, selected reaction monitoring; TOF, time-
of-flight.

DMD#81083

Abstract

11 β -hydroxysteroid dehydrogenase 1 (11 β -HSD1) is mainly distributed in the human liver with no detectable levels in the intestine or kidney based on a newly developed proteomic approach. 11 β -HSD1 is mostly membrane bound and retained in the liver microsomal fraction. Inter-individual variability of 11 β -HSD1 is relatively low with about a three-fold difference. A significant correlation was not observed between various demographic variables (ethnicity, gender, age, weight, smoking, and alcohol use) and 11 β -HSD1 protein expression or activity based on data from thirty-one donors. PF-915275 has been identified as a selective 11 β -HSD1 inhibitor with minimal effects on carbonyl reductase 1 and major cytochrome P450 enzymes. 11 β -HSD1 has been shown, for the first time, to be involved in doxorubicin metabolism accounting for approximately 30% of doxorubicinol formation in human hepatocytes.

DMD#81083

1. Introduction

11 β -hydroxysteroid dehydrogenase 1 (11 β -HSD1) belongs to the short-chain dehydrogenase/reductase superfamily. It is the only well-known microsomal enzyme that plays a significant role in metabolizing drugs containing carbonyls. 11 β -HSD1 acts as a NADPH-dependent reductase in intact cells, but is a bidirectional enzyme capable of both reductase (reduction) and dehydrogenase (oxidation) reactions in microsomes depending on the presence of the appropriate cofactors (NADPH for reduction or NADP⁺ for oxidation, Figure 1). The difference between 11 β -HSD1 activity in intact cells and microsomes is likely due to the accessibility of relevant cofactors to the enzyme. 11 β -HSD1 has a pivotal physiological role in transforming cortisone to cortisol (a stress hormone) that subsequently activates glucocorticoid receptors (Figure 1). 11 β -HSD2, on the other hand, is a unidirectional dehydrogenase that converts active cortisol to inactive cortisone. 11 β -HSD1 is a glycosylated protein that anchors at the luminal side of the endoplasmic reticulum via an N-terminal transmembrane domain. As NADPH is impermeable through the endoplasmic reticulum membrane, co-localization and interaction between 11 β -HSD1 and hexose-6-phosphate dehydrogenase provides a direct supply of NADPH for the reductase activity (Dzyakanchuk Anna et al., 2009). 11 β -HSD1 is involved in the metabolism of a number of clinically important drugs, such as benfluron, bupropion, ketoprofen, metyrapone, oracin, prednisolone and triadimefon, as well as certain toxicants (e.g., NNK, nicotine-derived nitrosamine ketone) (Molnari and Myers, 2012; Skarydova and Wsol, 2012; Malatkova and Wsol, 2014). Selective inhibitors of 11 β -HSD1 are promising agents for the treatment of type 2 diabetes and cardiovascular disease (Wang, 2006; Hale and Wang, 2008; Anderson and Walker,

DMD#81083

2013). The X-ray single crystal structure of 11 β -HSD1 has been solved, which aids the structure-based design of potent and selective inhibitors (Hosfield et al., 2005; Julian et al., 2008). 11 β -HSD1 is expressed mainly in the liver, but is also found in female reproductive tissues such as the placenta and ovaries (<http://www.proteinatlas.org/>). Studies have shown the upregulation of 11 β -HSD1 in the pharyngeal mucosa and placentas of smokers; but, the increase observed might be too small to lead to functional impact (Gronau et al., 2002; Huuskonen et al., 2008; Malatkova and Wsol, 2014). Since 11 β -HSD1 has significant functional overlap with a number of cytosolic reductases, such as carbonyl reductase 1 (CBR1) and aldo-keto reductases (AKRs), protein abundance data can provide useful insights on its contribution to clearance relative to other reductases. In this study, a proteomic approach has been developed and applied to quantify 11 β -HSD1 in human tissues for major clearance organs including liver, intestine, and kidney to better understand the tissue distribution of the enzyme at the protein level and its impact on drug clearance. To the best of our knowledge, this is the first proteomic approach to quantify 11 β -HSD1 at the protein level in human tissues. Inter-individual variability was also evaluated using human liver microsomes from thirty-one donors with diverse histories of tobacco and alcohol use to examine the potential for demographic effects on 11 β -HSD1 expression and activity. Relative expression factor (REF) and relative activity factor (RAF) were established to predict the contribution of 11 β -HSD1 to clearance using human recombinant 11 β -HSD1 (hr-11 β -HSD1). The 11 β -HSD1 protein quantification data and tissue distribution information can help to understand hepatic and non-hepatic contribution of the enzyme and to develop PBPK (physiological based pharmacokinetic) models for 11 β -HSD1-mediated clearance. The

DMD#81083

involvement of 11 β -HSD1 to doxorubicin (Adriamycin) metabolism was investigated.

Doxorubicin is one of the most cost effective and widely used anti-cancer drugs (Hofman et al., 2015). The cardio-toxic metabolite, doxorubicinol, is thought to be formed mostly by CBR1 with minor contributions from AKRs (Kassner et al., 2008). In this study we demonstrate, for the first time, the role of 11 β -HSD1 in metabolizing doxorubicin to generate the metabolite doxorubicinol.

DMD#81083

2. Materials and Methods

2.1. Materials

Pools of 3-12 donors (both male and female) of human intestine (prepared from duodenal and jejunal tissues), kidney cytosols and microsomes, and human liver microsomes of thirty-one individual donors were obtained from Xenotech (Kansas City, KS). The pooled human liver microsomes (50 donors of both male and female) and cynomolgus monkey intestine microsomes (338 donors of both male and female, used as a control matrix) were purchased from Corning (Tewksbury, MA). Human liver cytosols (16 donors of both male and female) and cryopreserved human hepatocytes (Lot # DCM, 10 donors) were from BioreclamationIVT (Baltimore, MD). hr-11 β -HSD1 was from OriGene Technologies (Catalog# TP312093, Lot # 021617, Rockville, MD) and Cayman Chemical (Catalog # 10007815, Lot # 0486950, Ann Arbor, MI). Stable isotope-labeled (purity >95% and isotopic purity >99%) peptides used as internal standards (IS) and standard peptides were purchased from New England Peptide (Gardner, MA). Peptide purity was determined by the vendor using HPLC-UV and identified by MS (mass spectrometry) analysis. Amino acid analysis was also performed by the vendor to determine net peptide content. Concentrations of synthesized peptides were corrected by purity data for quantitation. Rapigest SF was from Waters (Milford, MA) and MS-grade trypsin was purchased from Thermo Scientific (Guilford, CT). Cortisone, cortisol, doxorubicin, doxorubicinol and PF-915275 (CAS# 857290-04-1, N-(6-Amino-2-pyridinyl)-4'-cyano[1,1'-biphenyl]-4-sulfonamide) (Siu et al., 2009) were from Pfizer Global Material Management (Groton, CT). Iodoacetamide, dithiothreitol, and other chemicals were from Sigma-Aldrich (St. Louis, MO) unless specified otherwise.

DMD#81083

2.2. Peptide Mapping and Selection

2.2.1. Sample Preparation for Peptide Mapping and Selection

Peptide mapping and selection experiments were initially performed with 0.4 mg protein of pooled human liver microsomes (HLM) and hr-11 β -HSD1 protein standards. The samples were prepared using methods described previously (Hua et al., 2017). Briefly, the samples were mixed with 4 volumes of 50 mM ammonium bicarbonate buffer (pH 8.5) containing 0.1% Rapigest SF in a 1-mL 96-well LoBind plate (Eppendorf, Hauppauge, NY) and heated at ~80 °C for 5 minutes in a water bath (VWR, Radnor, PA). The proteins were reduced by 5 mM dithiothreitol at 37 °C for 30 minutes followed by incubation with 10 mM iodoacetamide for 30 minutes in the dark. The final solution was incubated with trypsin at 20:1 (protein/trypsin) ratio overnight at 37 °C under mild agitation. The tryptic peptide solution was acidified to pH<2 with formic acid and transferred to a clean 1-mL 96-well LoBind plate followed by brief centrifugation. Acetonitrile (20 μ L) was added to the samples and the final organic solvent was 5%.

2.2.2. LC-MS/MS Methods for Peptide Mapping and Selection

The LC-MS/MS methods for peptide mapping using information-dependent acquisition (IDA) and SWATHTM are summarized in Supplemental Material (Tables 1s and 2s). Briefly, 20 μ L of the digested samples were injected onto a BEH C18 column (XBridge 130Å, 100 x 2.1 mm, 2.5 μ m; Waters, Milford, MA) by the CTC PAL autosampler (Leap Technologies, Carrboro, NC). A triple Time-Of-Flight (TOF) 6600 mass spectrometer (Sciex, Toronto, Canada) was used for data acquisition. An IDA experiment was first

DMD#81083

performed to provide peptide identification using ProteinPilot™ Software 5.0 (Sciex, Toronto, Canada) with the Paragon database search algorithm (proteome library: Uniprot_Homo_sapiens, updated on 2015/02). Both biological modifications and amino acid substitutions were searched in “Thorough” mode. The samples were then subjected to SWATH™ acquisition on the same LC-triple TOF MS instrument. The resulting protein pilot.group file from IDA acquisition was used to generate the ion library to guide SWATH™ data processing. The digested samples were re-injected on an API 5500 (Sciex, Toronto, Canada) triple quadrupole MS in SRM (selected reaction monitoring) mode to evaluate the quantitation performance the peptides. Five peptides VLGLIDTETAMK, AVSGIVHMQAAPK, VIVTGASK, EYSVSR and FALDGFFSSIR (abbreviated as VLG, AVS, VIV, EYS and FAL, hereafter) were initially selected as probe peptides. Selection criteria for surrogate peptides were similar to those described previously (Balogh et al., 2013). High amino acid sequence coverage was achieved for hr-11β-HSD1 (81%) and HLM (53%) with a confidence level cutoff > 95%. The light and isotopic stable-labeled peptide standards were synthesized (Table 4) and used for further evaluation of stability, measurement accuracy and digestion efficiency. Final LC (liquid chromatography) separation and SRM conditions on triple quadrupole MS were fine-tuned with synthesized standards and are summarized in Supplemental Material (Table 3s) and Table 1.

2.3. Evaluation of Peptides and Optimization of Digestion Efficiency

2.3.1. Accuracy and Stability Evaluation

DMD#81083

The stability of the five selected peptides was evaluated in the presence and absence of HLM. In the stability experiments without HLM, 20 μ L of combined peptide solution (1 μ M each) in four replicates was used instead of HLM and incubated for 3, 5, 9, and 16 hours using the procedure described in the section *Sample Preparation for Peptide Mapping and Selection*. To evaluate peptide stability in HLM, HLM (0.4 mg total protein) was spiked with 5 μ L of combined peptide solution (16 μ M each of the five peptides) in four replicates and incubated using the same procedure as described above for 3, 5, 9, and 16 hours. HLM (0.4 mg protein) samples without peptides were also processed in parallel and used as baseline. Calibration curves were prepared by spiking combined peptide solution into digested control matrix (cynomolgus monkey intestine microsomes). Calibration curve preparation details are described in the section *Sample Preparation for 11 β -HSD1 Quantitation*. Quantification was performed against peptide calibration curves. Measurement accuracy for the spiked peptides was calculated by dividing the concentrations of the peptides in the spiked samples after subtracting the baseline by the nominal concentrations.

Since the final samples were acidified to below pH 2 after digestion and there is a wait time before injection for LC-MS/MS analysis, peptide stability was evaluated using these conditions. The digested control matrix was spiked with 10 μ L of 1 μ M combined solution of five peptides and acidified with formic acid to pH < 2. The solution was stored at room temperature in an autosampler and sampled at 0, 9, 30, and 34 hours in triplicate. The combined solution (10 μ L) of five isotope-labeled peptides at 0.25 μ M

DMD#81083

each was added to the samples before injection and used as internal standard (IS). Peak area ratio between analyte and IS was used for stability evaluation.

2.3.2. Digestion Efficiency

To obtain optimal trypsin digestion efficiency, digestion time was evaluated with pooled HLM (0.4 mg protein) in four replicates using the same procedure as described in the section *Sample Preparation for Peptide Mapping and Selection* for 3, 5, 9, and 16 hours. Calibration curves were prepared by spiking combined peptide solution into the digested control matrix. The details of preparing calibration curves are described in the section *Sample Preparation for 11 β -HSD1 Quantitation*. Results (pmol/mg protein) of individual peptides were calculated using the standard curves.

2.4. Sample Preparation for 11 β -HSD1 Quantitation

For quantitation, samples containing 0.4 mg protein were processed in triplicate using the same procedure as described in *Sample Preparation for Peptide Mapping and Selection*. The samples were tryptic digested for 9 hours. Pooled monkey intestine microsomes were used as control matrix for calibration curves. Stock solutions (200 μ M) of standard peptides and stable isotope-labeled peptides were individually prepared in dimethylformamide (DMF). For calibration curves, the combined standard solutions of the peptides were prepared in the range of 0.010 to 30 μ M in 1:1 DMF/water. 10 μ L of calibration standards were spiked into the digested control matrix and 10 μ L of the combined IS at 0.25 μ M in the same diluent were spiked into all the digested samples (except double blanks) after acidification. The standard curve quantitation range is

DMD#81083

equivalent to 0.25 to 750 pmol/mg protein, assuming complete digestion of 11 β -HSD1 in the sample matrix.

2.5. LC-MS/MS SRM Sample Analysis

LC-triple quadrupole MS in SRM mode was used to optimize digestion efficiency, evaluate peptide stability, and determine final 11 β -HSD1 concentration in sample matrix. Autosampler and LC-MS/MS methods are summarized in Supplemental Material (Table 3s) and Table 1. Analysis of the SRM data was performed using MultiQuantTM Software 2.1 (Sciex, Toronto, Canada).

2.6. Measurement of 11 β -HSD1 Activity in Different Matrices

Cortisone to cortisol formation was used as an 11 β -HSD1 specific reaction to evaluate enzyme activity in human intestine, kidney and liver microsomes (0.75 mg/mL) and cytosols (1 mg/mL), and hr-11 β -HSD1 (10 μ g/mL) at 1 μ M. The final dimethyl sulfoxide (DMSO) concentration was 0.03% and NADPH cofactor was 1.4 mM. The solution was incubated at 37°C for 1 h in a heating block (Boeckel Scientific, Feasterville-Trevose, PA). At appropriate time points, an aliquot of solution was removed and quenched with cold acetonitrile containing IS. Cortisol metabolite formation was quantified using LC-MS/MS via a standard curve. Intrinsic clearance was calculated based on the rate of cortisol metabolite formation. Duplicates or triplicates were used for each study. The LC mobile phases were as follows: (a) 0.1% formic acid in water and (b) 0.1% formic acid in acetonitrile. The solvent gradient was: 95% (a)/5% (b) for 0.3 min, 5% (a)/ 95% (b) from 0.3 to 1.30 min and held until 2.3 min, 95% (a)/5% (b) from 2.3 min to 2.31 min. The

DMD#81083

compounds were eluted from the column (Acquity C18, 1.7 μ m, 2.1 mm \times 50 mm; Waters, Milford, MA) at a flow rate of 0.5 mL/min. Samples (10 μ L) were injected using a CTC PAL autosampler (Leap Technologies, San Diego, CA) for analysis. Shimadzu HPLC AD30 pumps (Columbia, MD) connected to an AB Sciex (Foster City, CA) 5500 triple quadrupole mass spectrometer equipped with a TurboIonSpray source were used. Analyst 1.6.2 software (Applied Biosystems, Foster City, CA) was used for data collection, processing, and analysis. The IS for LC-MS/MS quantification was terfenadine. The MS conditions at positive ion SRM mode are: cortisol Q1 363.2, Q3 121.2, DP 60, CE 60 and terfenadine Q1 472.2, Q3 436.3, DP 60, CE 60.

2.7. Evaluation of the Role of 11 β -HSD1 in Doxorubicin Metabolism

Doxorubicin (100 μ M) was incubated with hr-11 β -HSD1 (100 μ g/mL, from both Cayman Chemical and OriGene Technologies) with final DMSO concentration of 1% and NADPH cofactor of 1.4 mM at 37 $^{\circ}$ C for 1 h in a heating block in duplicate. Samples without the addition of NADPH were used as negative controls. At appropriate time points, an aliquot of solution was removed and quenched with cold acetonitrile containing IS. Doxorubicinol reduction metabolite formation was quantified using LC-MS/MS in positive ion SRM mode with Q1 546, Q3 363, DP 60, CE 30.

2.8. Evaluation of Concentration and Selectivity for 11 β -HSD1 Inhibitor PF-915275

The inhibitory concentration of 11 β -HSD1 inhibitor, PF-915275, was determined in cryopreserved human hepatocytes at 0.5 million cells/mL using cortisone as a substrate (1 μ M) and via monitoring cortisol formation (see above for LC-MS/MS conditions).

DMD#81083

Detailed protocols on cytochrome P450 (CYP) selectivity determination have been reported previously (Yang et al., 2016). Briefly, human hepatocytes (0.5 million cells/mL) were incubated with PF-915275 at 1 μ M in the presence of probe substrates at 1 μ M. The following specific substrate reactions were monitored with and without 11 β -HSD1 inhibitor PF-915275 at 1 μ M to evaluate the selectivity against several CYPs: phenacetin (1A2) to acetaminophen, bupropion (2B6) to OH-bupropion, paclitaxel (2C8) to 6 α -OH-paclitaxel, diclofenac (2C9) to 4'-OH-diclofenac, S-mephenytoin (2C19) to 4'-OH-S-mephenytoin, dextromethorphan (2D6) to dextrorphan, and midazolam (3A) to 1'-OH-midazolam. Metabolite formation was monitored over one hour and used to calculate % inhibition of the enzymes. Selectivity of PF-915275 (1 μ M) against CBR1 was conducted using doxorubicin as a substrate (1 μ M) in hr-CBR1 (human recombinant CBR1, 10 μ g/mL) and monitored for the formation of doxorubicinol over a one-hour incubation. Because a specific CBR1 substrate reaction is currently not available, hr-CBR1 was used to evaluate PF-915275 selectivity against CBR1.

2.9. Determination of 11 β -HSD1 Contribution to Doxorubicin Metabolism

Doxorubicin (1 μ M) was incubated with cryopreserved human hepatocytes at 0.5 or 2 million cells/mL with and without the presence of 11 β -HSD1 inhibitor PF-915275 at 1 μ M. The incubation was done at 37 °C in a CO₂ incubator (5% CO₂/95% air) with 75% relative humidity on an orbital shaker (VWR, Radnor, NJ) at 150 rpm for 4 hours. At various time points, samples were taken and quenched with cold acetonitrile containing IS. The solution was centrifuged and the supernatant was transferred to a clean plate and injected to LC-MS/MS for analysis. Doxorubicinol metabolite formation was used to

DMD#81083

evaluate the contribution of 11β -HSD1 to doxorubicin reduction (see above for MS conditions). Percent inhibition was calculated using the initial slope of the doxorubicinol metabolite formation curve with and without the inhibitor. The studies of 11β -HSD1 contribution to doxorubicin reduction were performed on five different days in duplicate and the average of all the data was reported.

DMD#81083

3. Results

This is the first study reporting 11 β -HSD1 protein expression in human intestine, kidney and liver using a newly developed proteomic approach. The selection criteria for the surrogate peptides for protein quantification include that they are unique within the human proteome, have 6-20 amino acid residues, and have no known post-translational modifications, single nucleotide polymorphisms, labile amino acids or missed cleavage sites. Five surrogate peptides meeting the criteria were selected for further evaluation of stability and digestion efficiency (Table 1). Peptide amounts (in pmol/mg protein) at different time points were quantitated using calibration curves to evaluate stability and digestion efficiency. It is important to use the quantified amount instead of MS response for these evaluations as the MS response indicates only the relative stability or completeness of digestion rather than the absolute amount. Peptide bonds can be cleaved with a wide range of rates during digestion and the ability of enzymes to cleave different scissible bonds varies (Slechtova et al., 2015), even when the reaction time is sufficient. The stability of the five selected peptides under tryptic digestion conditions were examined in the presence and absence of HLM. The results showed that all five peptides were stable without HLM for at least 16 hours with 90 - 110% remaining (Table 4s in Supplemental Material). These data suggest that the peptides had good chemical stable and no significant observable loss. In the presence of HLM, all the peptides had stability \geq 87% at 9 hours with the exception of FLA (Table 5s in Supplemental Material). FLA had 40% remaining at 9 hours and was too unstable to be used as a surrogate peptide for quantitation.

DMD#81083

Ideally, the concentration for each of the cleaved peptides should be the same after digestion is complete. However, due to different cleavage rates, accessibility of scissible bonds, chemical/physical peptide stability, etc., the peptide concentrations detected by LC-MS/MS after digestion are often different and the peptides providing the highest concentration should be used as surrogate peptides for protein quantitation. For the digested samples of 11 β -HSD1, the peptide concentrations for VLG, EYS, and FLA were significantly lower than for AVS and VIV (Figure 2). VLG had the lowest digestion efficiency and was not suitable as a surrogate peptide even though it demonstrated good stability. FAL decreased significantly after 5 hours due to instability. EYS concentration increased over the 16 hour digestion period. It offered attractive properties as a surrogate peptide for quantitation but longer digestion times (>16 hrs) would be needed. AVS and VIV had the highest measured concentrations with comparable results at both 9 and 16 hours of digestion. Both demonstrated acceptable stability during the digestion process (\geq 87% remaining after 9 hours) and were therefore selected as surrogate peptides for quantitation. Overall, the 9 hour digestion period offered the maximum efficiency for the AVS and VIV peptides and was used for subsequent sample preparation (Figure 2). Stability under autosample storage conditions was also examined at room temperature in solution with pH <2. AVS and VIV were both stable over 34 hours (<5% change, data not shown), suggesting the lack of instability concerns for these peptides stored in the autosampler prior to analysis.

11 β -HSD1 protein abundance was measured in both cytosols and microsomes of human intestine, kidney, and liver using both AVS and VIV peptides (Table 2). The two

DMD#81083

surrogate peptides showed linear response over the concentration range of 0.25 to 750 pmol/protein. In control matrix (cynomolgus monkey intestine microsomes), no interference peak was found for AVS and the signals were less than 20% of the LOQ (lower limit of quantitation) for VIV. These data suggested that 11 β -HSD1 was not present in human intestine and kidney, while high abundance was found in HLM with 62 pmol/mg protein for a pooled lot of fifty donors. Only trace amounts were detected in liver cytosol (3.5 pmol/mg protein), a result potentially due to contamination from the microsomal fraction during fractionation of the liver samples. For the three clearance organs examined, 11 β -HSD1 appears to only be expressed in liver with a significant amount as a membrane bound protein. 11 β -HSD1 abundance in HLM from thirty-one donors was also quantified to explore inter-individual variability and demographic effects (Table 2). 11 β -HSD1 protein amounts ranged from 36-109 pmol/mg protein suggesting relatively small inter-individual variability of approximately 3-fold. The demographic information (e.g., ethnicity, gender, age, weight, smoking, and alcohol use) of the individual liver donors is included in the Supplemental Material (Table 6s). Using a variety of exploratory statistical analyses, e.g., t-test, 1-way ANOVA, both simple and multiple regressions, we did not obtain robust evidence of statistically significant effects between the demographic variables and 11 β -HSD1 abundance or intrinsic clearance (results not shown). For hr-11 β -HSD1, the amounts were 4161 and 5686 pmol/mg protein for the materials from OriGene Technologies and Cayman Chemical, respectively. The REF values based on both lots of hr-11 β -HSD1 are summarized in Table 3.

DMD#81083

11 β -HSD1 catalytic activity was measured using cortisone as a substrate and monitored for cortisol metabolite formation. The rate of cortisol formation is summarized in Table 2. The intrinsic clearance values range from 8.7 to 30 μ L/min/mg in pooled or individual HLM donors. The intrinsic clearance in human hepatocytes was also determined to be 6.2 ± 0.22 μ L/min/million cells or 15.6 ± 0.55 mL/min/kg, an estimate comparable to the scaled HLM value in the pooled lot (HLM/102), i.e., 21.5 mL/min/kg. The inter-individual variability of 11 β -HSD1 based on functional activity of cortisone reduction is approximately 3-fold, a relatively small value and in line with those based on protein expression. The 11 β -HSD1 activity of the hr-11 β -HSD1 is 3642 μ L/min/mg for the OriGene Technologies lot and 236 μ L/min/mg for the Cayman Chemical lot. Even though the protein levels are similar for both vendors, the 11 β -HSD1 activity is 15-fold higher for the material from OriGene Technologies relative to Cayman Chemical. The correlation between 11 β -HSD1 protein abundance and activity was poor ($R^2 = 0.066$, Figure 3A) when using HLM data only, a result potentially due to a narrow data range (~3-fold). However, with the addition of HLC (human liver cytosol) and hr-11 β -HSD1 data, in an effort to increase the spread of these data over multiple log units, 11 β -HSD1 protein abundance and activity now appear correlated ($R^2 = 0.82$, Figure 3B). The RAF values based on both lots of hr-11 β -HSD1 and both HLM and HHEP are summarized in Table 3.

With our improved understanding of tissue distribution, the contribution of 11 β -HSD1 to the formation of the doxorubicinol metabolite from doxorubicin was investigated.

Doxorubicinol metabolite formulation was reported in the literature to be mostly

DMD#81083

mediated by CBR1 with minor contribution from AKRs (Kassner et al., 2008).

Incubation of doxorubicin with hr-11 β -HSD1 from Cayman Chemical indicated doxorubicinol metabolite formation (Figure 4). Formation of doxorubicinol metabolite was also observed using hr-11 β -HSD1 from OriGene Technology (data not shown), suggesting for the first time that 11 β -HSD1 is involved in the metabolism of doxorubicin to the metabolite doxorubicinol. These results were further verified using HHEP by monitoring doxorubicinol metabolite formation with and without 11 β -HSD1 inhibitor PF-915275. PF-915275 has been reported to be a highly potent inhibitor for 11 β -HSD1 (Siu et al., 2009). The selectivity of PF-915275 against a variety of CYPs and CBR1 was evaluated using HHEP (Figure 5). PF-915275 at 1 μ M was not only a potent inhibitor of 11 β -HSD1 (89%) but was also selective against CBR1 and the major CYPs with only a minor inhibition of CYP2C19 (29%). The contribution of 11 β -HSD1 to doxorubicinol formation was $29\% \pm 7.9\%$ based on metabolite formation in HHEP with and without inhibitor PF-915275 (Table 4). Because doxorubicin does not have significant turnover in human hepatocytes, the intrinsic clearance is not measurable. Therefore, REF and RAF approaches or metabolite formation rate were not applied to estimate the percent contribution to clearance by 11 β -HSD1.

DMD#81083

Discussion

This paper reported the first study to quantify 11 β -HSD1 levels using a newly developed proteomic approach. Tissue distribution of 11 β -HSD1 is predominately in the human liver microsomal fraction with a moderate concentration (60 pmol/mg protein) similar to CYP2C9 (72 pmol/mg protein) in the liver (SIMCYP[®] database). 11 β -HSD1 was not detectable in the intestine and kidney, indicating the critical physiological role for this enzyme in the liver for conversion of cortisone to cortisol. The inter-individual variability of 11 β -HSD1 was approximately 3-fold based on both protein levels and enzymatic activity. This variability is quite small suggesting that the enzyme is highly regulated, a hypothesis consistent with the important physiological function of the enzyme in converting inactive cortisone to active cortisol, a stress hormone known to activate glucocorticoid receptors. Due to the relatively narrow protein distribution of 11 β -HSD1 in the liver for the individual donors, the correlation between protein amount and enzyme activity was not observed. But, when the distribution range is increased by adding HLC and hr-11 β -HSD1 data, a correlation was observed between protein expression and 11 β -HSD1 activity. Various available demographic factors, such as ethnicity, gender, age, weight, smoking, and alcohol use, did not appear to impact 11 β -HSD1 activity based on this study, although the sample size was relatively small and the sample demographic distribution was not evenly balanced or represented in the various groups. Tobacco use has been reported to up-regulate 11 β -HSD1 expression in the pharyngeal mucosa and placentas of smokers, though no functional changes have been observed (Gronau et al., 2002; Huuskonen et al., 2008; Malatkova and Wsol, 2014). The impact of smoking on liver 11 β -HSD1 levels has not been reported. In this study,

DMD#81083

significant statistical differences were not observed between smokers and non-smokers using either 11 β -HSD1 protein expression or activity. The protein quantification and activity data are useful to estimate the contribution of the enzyme to clearance through REF and RAF values when selective inhibitors are not available. This approach is not applied to the doxorubicin case in this study due to no significant turnover of the parent in the in vitro systems. Tissue abundance information is beneficial for development of PBPK models to predict human pharmacokinetics and drug-drug interaction potential.

Doxorubicin is one of the most effective chemotherapeutic agents and it has become the “gold standard” for the treatment of various cancers, such as haematological (lymphomas) and solid breast, ovarian, lung and liver tumors (Hofman et al., 2015). Almost 60% children diagnosed with cancer receive anthracyclines (e.g., doxorubicin) as part of their treatment (Voeller et al., 2015). However, its effectiveness is limited by a cumulative dose-dependent cardio-toxicity that can result in irreversible heart failure (Volkova and Russell, 2011). Several mechanisms have been proposed for doxorubicin toxicity. One mechanism is that the metabolite from doxorubicin reduction, i.e., doxorubicinol, induces heart failure (Olson et al., 1988; Forrest and Gonzalez, 2000; Forrest et al., 2000; Miura et al., 2013), a mechanism that has also been shown to cause resistance in tumors (Hofman et al., 2015). The reductases involved in this biotransformation have been shown to be mainly mediated by CBR1 and AKRs (Kassner et al., 2008; Bains et al., 2010). Inhibitors of CBR1 are currently being developed to improve the therapeutic index of doxorubicin by decreasing the formation of the doxorubicinol metabolite (Hu et al., 2015; Shi and Di, 2017). We demonstrated for the

DMD#81083

first time in this study that 11 β -HSD1 is also involved in catalyzing the conversion of doxorubicin to doxorubicinol and that it is a significant pathway accounting for approximately 30% of doxorubicinol formation. The functional redundancy of reductases (CBR1, AKRs, 11 β -HSD1) provides multiple pathways to enhance the chance for elimination of the intrinsically reactive ketones and aldehydes (Shi and Di, 2017). Selective inhibitor of 11 β -HSD1, PF-915275, has also been identified in this study, which enables the determination of the enzyme contribution to metabolism. Owing to the advances and availability of the recombinant enzyme and the selective inhibitor, we were able to discover new clearance pathway for doxorubicin, which has been on the market for more than 40 years and is one of the most widely prescribed anticancer drugs.

Authorship Contributions

Participated in research design: Yang, Hua, Ryu, Yates, Chang, Zhang, Di.

Conducted experiments: Yang, Hua, Ryu.

Performed data analysis: Yang, Hua, Ryu, Yates, Chang, Zhang, Di.

Wrote or contributed to the writing of the manuscript: Yang, Hua, Ryu, Yates, Zhang, Di.

DMD#81083

References

- Anderson A and Walker BR (2013) 11 β -HSD1 Inhibitors for the Treatment of Type 2 Diabetes and Cardiovascular Disease. *Drugs* **73**:1385-1393.
- Bains OS, Grigliatti TA, Reid RE, and Riggs KW (2010) Naturally occurring variants of human aldo-keto reductases with reduced in vitro metabolism of daunorubicin and doxorubicin. *J Pharmacol Exp Ther* **335**:533-545.
- Balogh LM, Kimoto E, Chupka J, Zhang H, and Lai Y (2013) Membrane protein quantification by peptide-based mass spectrometry approaches: studies on the organic anion-transporting polypeptide family. *Journal of Proteomics & Bioinformatics* **6**:229-236.
- Dzyakanchuk Anna A, Balazs Z, Nashev Lyubomir G, Amrein Kurt E, and Odermatt A (2009) 11beta-Hydroxysteroid dehydrogenase 1 reductase activity is dependent on a high ratio of NADPH/NADP(+) and is stimulated by extracellular glucose. *Molecular and cellular endocrinology* **301**:137-141.
- Forrest GL and Gonzalez B (2000) Carbonyl reductase. *Chemico-Biological Interactions* **129**:21-40.
- Forrest GL, Gonzalez B, Tseng W, Li X, and Mann J (2000) Human carbonyl reductase overexpression in the heart advances the development of doxorubicin-induced cardiotoxicity in transgenic mice. *Cancer Research* **60**:5158-5164.
- Gronau S, Koenig Greger D, Jerg M, and Riechelmann H (2002) 11Beta-hydroxysteroid dehydrogenase 1 expression in squamous cell carcinomas of the head and neck. *Clinical otolaryngology and allied sciences* **27**:453-457.
- Hale C and Wang M (2008) Development of 11 β -HSD1 inhibitors for the treatment of type 2 diabetes. *Mini-Reviews in Medicinal Chemistry* **8**:702-710.
- Hofman J, Skarka A, Havrankova J, and Wsol V (2015) Pharmacokinetic interactions of breast cancer chemotherapeutics with human doxorubicin reductases. *Biochemical Pharmacology (Amsterdam, Netherlands)* **96**:168-178.
- Hosfield DJ, Wu Y, Skene RJ, Hilgers M, Jennings A, Snell GP, and Aertgeerts K (2005) Conformational Flexibility in Crystal Structures of Human 11 β -Hydroxysteroid Dehydrogenase Type I Provide Insights into Glucocorticoid Interconversion and Enzyme Regulation. *Journal of Biological Chemistry* **280**:4639-4648.
<http://www.proteinatlas.org/>.
- Hu D, Miyagi N, Arai Y, Oguri H, Miura T, Nishinaka T, Terada T, Gouda H, El-Kabbani O, Xia S, Toyooka N, Hara A, Matsunaga T, Ikari A, and Endo S (2015) Synthesis of 8-hydroxy-2-iminochromene derivatives as selective and potent inhibitors of human carbonyl reductase 1. *Organic & Biomolecular Chemistry* **13**:7487-7499.
- Hua W, Zhang H, Ryu S, Yang X, and Di L (2017) Human Tissue Distribution of Carbonyl Reductase 1 Using Proteomic Approach With Liquid Chromatography-Tandem Mass Spectrometry. *J Pharm Sci* **106**:1405-1411.
- Huuskonen P, Storvik M, Reinisalo M, Honkakoski P, Rysae J, Hakkola J, and Pasanen M (2008) Microarray analysis of the global alterations in the gene expression in the placentas from cigarette-smoking mothers. *Clin Pharmacol Ther (N Y, NY, U S)* **83**:542-550.
- Julian LD, Wang Z, Bostick T, Caille S, Choi R, DeGraffenreid M, Di Y, He X, Hungate RW, Jaen JC, Liu J, Monshouwer M, McMinn D, Rew Y, Sudom A, Sun D, Tu

DMD#81083

- H, Ursu S, Walker N, Yan X, Ye Q, and Powers JP (2008) Discovery of Novel, Potent Benzamide Inhibitors of 11 β -Hydroxysteroid Dehydrogenase Type 1 (11 β -HSD1) Exhibiting Oral Activity in an Enzyme Inhibition ex Vivo Model. *J Med Chem* **51**:3953-3960.
- Kassner N, Huse K, Martin H-J, Goedel-Armbrust U, Metzger A, Meineke I, Brockmoeller J, Klein K, Zanger UM, Maser E, and Wojnowski L (2008) Carbonyl reductase 1 is a predominant doxorubicin reductase in the human liver. *Drug Metab Dispos* **36**:2113-2120.
- Malatkova P and Wsol V (2014) Carbonyl reduction pathways in drug metabolism. *Drug Metabolism Reviews* **46**:96-123.
- Miura T, Taketomi A, Nishinaka T, and Terada T (2013) Regulation of human carbonyl reductase 1 (CBR1, SDR21C1) gene by transcription factor Nrf2. *Chemico-Biological Interactions* **202**:126-135.
- Molnari JC and Myers AL (2012) Carbonyl reduction of bupropion in human liver. *Xenobiotica* **42**:550-561.
- Olson RD, Mushlin PS, Brenner DE, Fleischer S, Cusack BJ, Chang BK, and Boucek RJ, Jr. (1988) Doxorubicin cardiotoxicity may be caused by its metabolite, doxorubicinol. *Proc Natl Acad Sci U S A* **85**:3585-3589.
- Shi SM and Di L (2017) The role of carbonyl reductase 1 in drug discovery and development. *Expert Opin Drug Metab Toxicol* **13**:859-870.
- Siu M, Johnson Theodore O, Wang Y, Nair Sajiv K, Taylor Wendy D, Cripps Stephan J, Matthews Jean J, Edwards Martin P, Pauly Thomas A, Ermolieff J, Castro A, Hosea Natilie A, LaPaglia A, Fanjul Andrea N, and Vogel Jennifer E (2009) N-(Pyridin-2-yl) arylsulfonamide inhibitors of 11beta-hydroxysteroid dehydrogenase type 1: Discovery of PF-915275. *Bioorg Med Chem Lett* **19**:3493-3497.
- Skarydova L and Wsol V (2012) Human microsomal carbonyl reducing enzymes in the metabolism of xenobiotics: well-known and promising members of the SDR superfamily. *Drug Metabolism Reviews* **44**:173-191.
- Slechtova T, Gilar M, Kalikova K, and Tesarova E (2015) Insight into Trypsin Miscalculation: Comparison of Kinetic Constants of Problematic Peptide Sequences. *Analytical Chemistry (Washington, DC, United States)* **87**:7636-7643.
- Voeller S, Boos J, Krischke M, Wuerthwein G, Kontny NE, Boddy AV, and Hempel G (2015) Age-Dependent Pharmacokinetics of Doxorubicin in Children with Cancer. *Clin Pharmacokinet* **54**:1139-1149.
- Volkova M and Russell R (2011) Anthracycline cardiotoxicity: prevalence, pathogenesis and treatment. *Current Cardiology Reviews* **7**:214-220.
- Wang M (2006) Inhibitors of 11beta-hydroxysteroid dehydrogenase type 1 for the treatment of metabolic syndrome. *Current opinion in investigational drugs (London, England : 2000)* **7**:319-323.
- Yang X, Atkinson K, and Di L (2016) Novel Cytochrome P450 Reaction Phenotyping for Low-Clearance Compounds Using the Hepatocyte Relay Method. *Drug Metab Dispos* **44**:460-465.

DMD#81083

Legend for Figures

Figure 1. Interconversion between cortisone and cortisol catalyzed by 11 β -HSD1 and 11 β -HSD2. In intact cells, 11 β -HSD1 metabolizes cortisone to cortisol using NADPH and generates NADP⁺. In microsomes, 11 β -HSD1 catalyzes the bidirectional reaction depending on the cofactors available. In the presence of NADPH, 11 β -HSD1 reduces cortisone to cortisol. In the presence of NADP⁺, 11 β -HSD1 oxidizes cortisol to cortisone. 11 β -HSD2 is a unidirectional enzyme that oxidizes cortisol to cortisone using NAD⁺ cofactor and generates NADH.

Figure 2. Digestion Efficiency of 11 β -HSD1 in Human Liver Microsomes.

Figure 3. Protein Abundance and Intrinsic Clearance Correlation for 11 β -HSD1. (A)

Data from HLM only; (B) Data includes HLM, HLC and hr-11 β -HSD1 enzyme.

Figure 4. Formation of Doxorubicinol in hr- 11 β -HSD1 With and Without NADPH

Figure 5. 11 β -HSD1 Inhibitor PF-915275 Selectivity Against CYP and CBR1 Enzymes

DMD#81083

Table 1. MS Method for Peptide Analysis using SRM Acquisition

Mass Spectrometer	Sciex API-5500-Electrospray (+)	
Data collection software/version	Analyst 1.6, MultiQuant 2.1.	
Ion source temperature	650 °C	
IonSpray voltage	5000 V	
Declustering potential	80 V	
Dwell time	20 ms	
SMR transitions (and collisional energy settings)	H2N-VLGLIDTETAMK-OH	m/z 645.9→ m/z 1078.5 (20 eV) ^c
	H2N-AVSGIVHMQAAPK-OH	m/z 436.9→ m/z 569.9 (20 eV) ^c
	H2N-VIVTGASK-OH	m/z 387.8→ m/z 562.5 (22 eV) ^c
	H2N-EYSVSR-OH	m/z 370.8→ m/z 448.4 (25 eV) ^c
	H2N-FALDGFFSSIR-OH	m/z 630.3→ m/z 928.4 (23 eV) ^c
	H2N-VLGLIDTETAMK [^] -OH (IS) ^a	m/z 649.9→ m/z 1086.5 (20 eV) ^c
	H2N-AVSGIVHMQAAPK [^] -OH (IS) ^a	m/z 439.6→ m/z 573.9 (20 eV) ^c
	H2N-VIVTGASK [^] -OH (IS) ^a	m/z 391.8→ m/z 570.5 (22 eV) ^c
	H2N-EYSVSR [^] -OH (IS) ^b	m/z 375.8→ m/z 458.4 (25 eV) ^c
	H2N-FALDGFFSSIR [^] -OH (IS) ^b	m/z 635.3→ m/z 938.4 (23 eV) ^c

^a: K[^]--Internal standard peptides were labeled at C-terminal arginine (K)=(¹³C)₆H₁₄(¹⁵N)₂O₂ (mass shift+8)

^b: R[^]--Internal standard peptides were labeled at C-terminal arginine (R)=(¹³C)₆H₁₄(¹⁵N)₄O₂ (mass shift+10)

^c: Collision energy

DMD#81083

Table 2. 11 β -HSD1 Protein Abundance in Individual/Pooled Human Liver, Intestine, and Kidney Cytosols and Microsomes (n=3)

Tissues/Lot	11 β -HSD1 Protein Concentration (pmol/mg protein) \pm SD ^a			Intrinsic clearance (μ L/min/mg)
	Based on AVS peptide probe	Based on VIV peptide probe	Average based on both AVS and VIV	
Pooled HIC	<LOQ ^b	<LOQ	<LOQ	ND
Pooled HIM	<LOQ	<LOQ	<LOQ	ND
Pooled HKC	<LOQ	<LOQ	<LOQ	0.1 \pm 0.04
Pooled HKM	<LOQ	<LOQ	<LOQ	0.2 \pm 0.11
Pooled HLC	3.06 \pm 0.07	4.09 \pm 0.13	3.47 \pm 0.09	0.5 \pm 0.12
Pooled HLM/102	50.7 \pm 6.7	72.7 \pm 8.6	61.7 \pm 7.6	22.8 \pm 0.075 ^c
HLM/262	75.8 \pm 12.3	96.4 \pm 7.3	86.1 \pm 9.8	17.5 \pm 1.3
HLM/375	30.4 \pm 0.4	44.3 \pm 0.6	37.3 \pm 0.5	19.8 \pm 3.2
HLM/377	32.6 \pm 0.6	48.4 \pm 2.2	40.5 \pm 1.4	15.5 \pm 2.0
HLM/380	67.5 \pm 1.1	89.9 \pm 3.2	78.7 \pm 2.1	25.9 \pm 2.1
HLM/384	60.3 \pm 2.5	88.0 \pm 0.6	74.2 \pm 1.5	21.5 \pm 2.2
HLM/402	41.0 \pm 3.0	57.8 \pm 4.1	49.4 \pm 3.6	23.5 \pm 2.3
HLM/403	44.7 \pm 4.5	54.1 \pm 5.0	49.4 \pm 4.7	8.71 \pm 1.5
HLM/405	37.8 \pm 4.5	50.7 \pm 6.8	44.3 \pm 5.6	16.7 \pm 2.7
HLM/406	29.0 \pm 4.6	43.6 \pm 5.5	36.3 \pm 5.0	16.4 \pm 1.2
HLM/418	59.4 \pm 8.7	82.1 \pm 11.5	70.8 \pm 10.1	26.5 \pm 0.66
HLM/421	97.6 \pm 9.0	122 \pm 13	109 \pm 11	22.7 \pm 0.49
HLM/439	59.9 \pm 3.1	81.3 \pm 10.5	70.6 \pm 6.4	22.8 \pm 1.8
HLM/448	38.6 \pm 3.4	53.8 \pm 1.8	46.2 \pm 1.2	15.2 \pm 0.50
HLM/467	31.6 \pm 1.1	41.2 \pm 1.5	36.4 \pm 1.3	13.7 \pm 0.55
HLM/469	49.2 \pm 6.3	72.9 \pm 5.8	61.0 \pm 6.0	16.2 \pm 0.55
HLM/486	73.0 \pm 2.0	92.4 \pm 2.6	82.7 \pm 2.0	20.0 \pm 0.44
HLM/494	54.1 \pm 3.9	69.3 \pm 7.0	61.7 \pm 5.5	18.1 \pm 0.37
HLM/499	46.0 \pm 1.6	64.9 \pm 1.9	55.5 \pm 1.6	18.8 \pm 1.9
HLM/508	51.4 \pm 9.0	74.2 \pm 9.8	62.8 \pm 9.4	16.6 \pm 0.78
HLM/510	34.7 \pm 1.2	51.3 \pm 3.1	43.0 \pm 2.1	15.7 \pm 0.38
HLM/512	47.9 \pm 2.3	63.6 \pm 1.7	55.8 \pm 1.6	26.5 \pm 0.75
HLM/523	51.5 \pm 5.6	69.0 \pm 8.9	60.3 \pm 7.2	19.5 \pm 0.31
HLM/532	58.9 \pm 7.5	77.1 \pm 9.2	68.0 \pm 8.4	23.3 \pm 1.1
HLM/535	41.0 \pm 7.1	56.9 \pm 9.4	49.0 \pm 8.3	23.6 \pm 0.21
HLM/552	83.5 \pm 16.4	104 \pm 18	93.6 \pm 17.1	17.3 \pm 0.41
HLM/556	49.0 \pm 6.8	72.0 \pm 6.6	60.5 \pm 6.2	20.9 \pm 0.85
HLM/566	38.9 \pm 11.1	53.9 \pm 8.9	46.4 \pm 10.0	29.9 \pm 0.11
HLM/573	68.1 \pm 4.4	84.0 \pm 7.9	76.0 \pm 6.1	20.3 \pm 1.2
HLM/751	64.0 \pm 6.9	84.4 \pm 7.7	74.2 \pm 7.3	18.4 \pm 1.5
HLM/838	55.4 \pm 6.8	76.5 \pm 8.1	65.9 \pm 7.4	16.8 \pm 3.5
HLM/843	77.1 \pm 11.2	104 \pm 19	90.7 \pm 15.2	15.3 \pm 0.34
Human recombinant 11 β -HSD1 (OriGene)	4600 \pm 130	3723 \pm 224	4161 \pm 176	3642 \pm 37
Human recombinant 11 β -HSD1 (Cayman)	6490 \pm 646	4882 \pm 453	5686 \pm 539	236 \pm 21

^a: Data generated from 3 replicates of each sample

^b: LOQ is 0.25 pmol/mg protein

^c: Intrinsic clearance in human hepatocytes is determined to be 6.2 \pm 0.22 μ L/min/million cells or 15.6 \pm 0.55 mL/min/kg, a value comparable to scaled HLM data, i.e., 21.5 mL/min/kg.

DMD#81083

Table 3. RAF and REF Values for Human Recombinant 11 β -HSD1

Human recombinant 11 β -HSD1 Vendor, Lot	RAF based on human liver microsomes	RAF based on human hepatocytes	REF based on human liver microsomes
OriGene, Lot # 021617	0.0063	0.0045	0.015
Cayman, Lot # 0486950	0.097	0.070	0.011

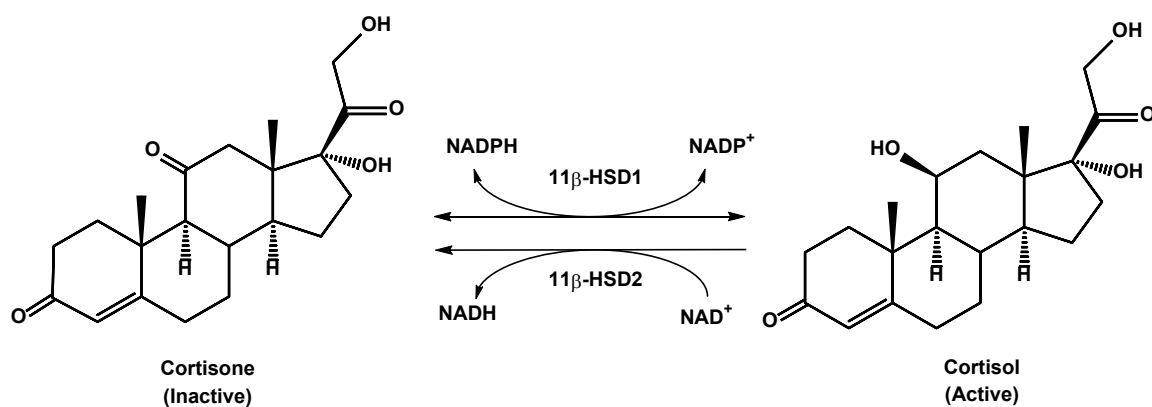
DMD#81083

**Table 4. Percent Inhibition of Doxorubicinol Formation in Human Hepatocytes
Using Selective 11 β -HSD1 Inhibitor PF-915275**

Experiments	Cell Density (Million Cells/mL)	% Inhibition of Doxorubicinol Formation
1	2	29
2	2	28
3	0.5	27
4	0.5	41
5	2	19
	Average and Standard Deviation	29 \pm 7.9

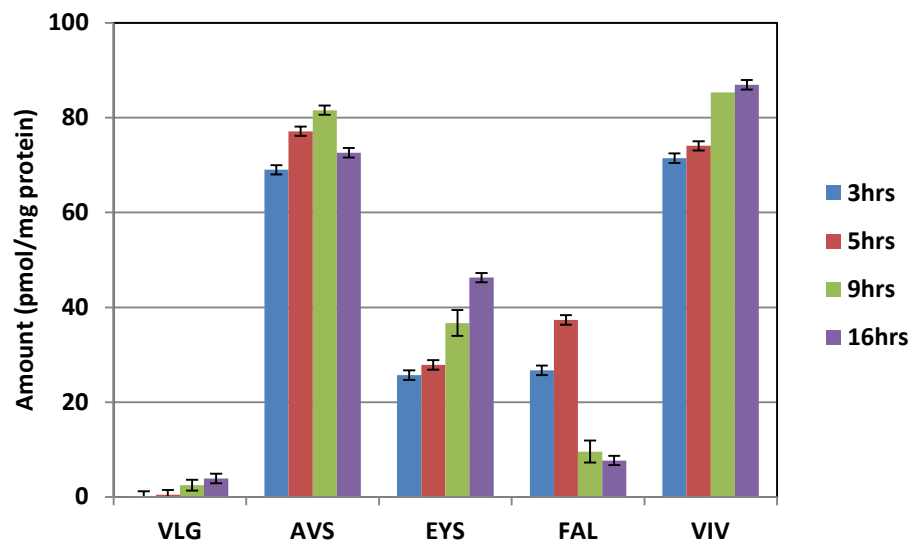
DMD#81083

Figure 1.



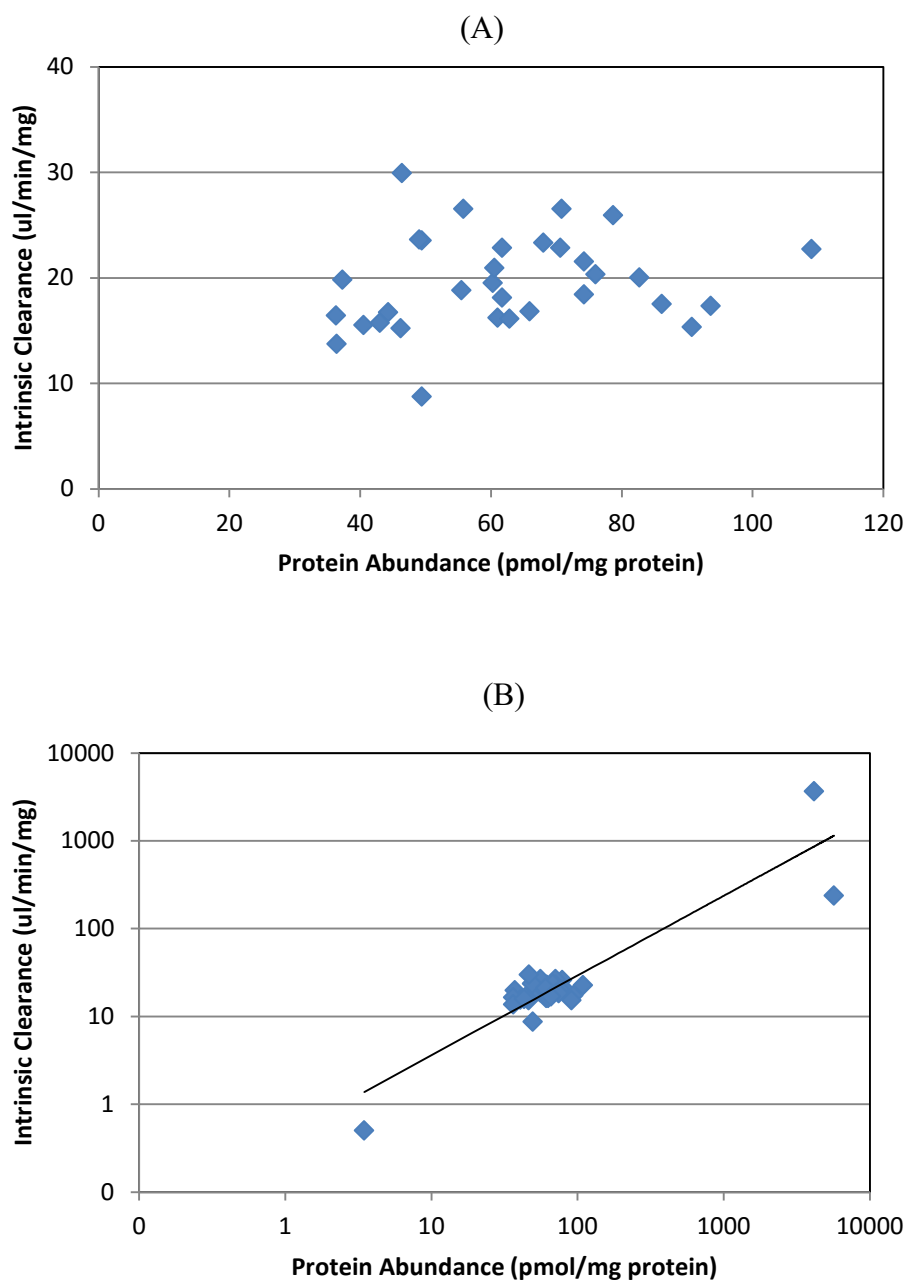
DMD#81083

Figure 2.



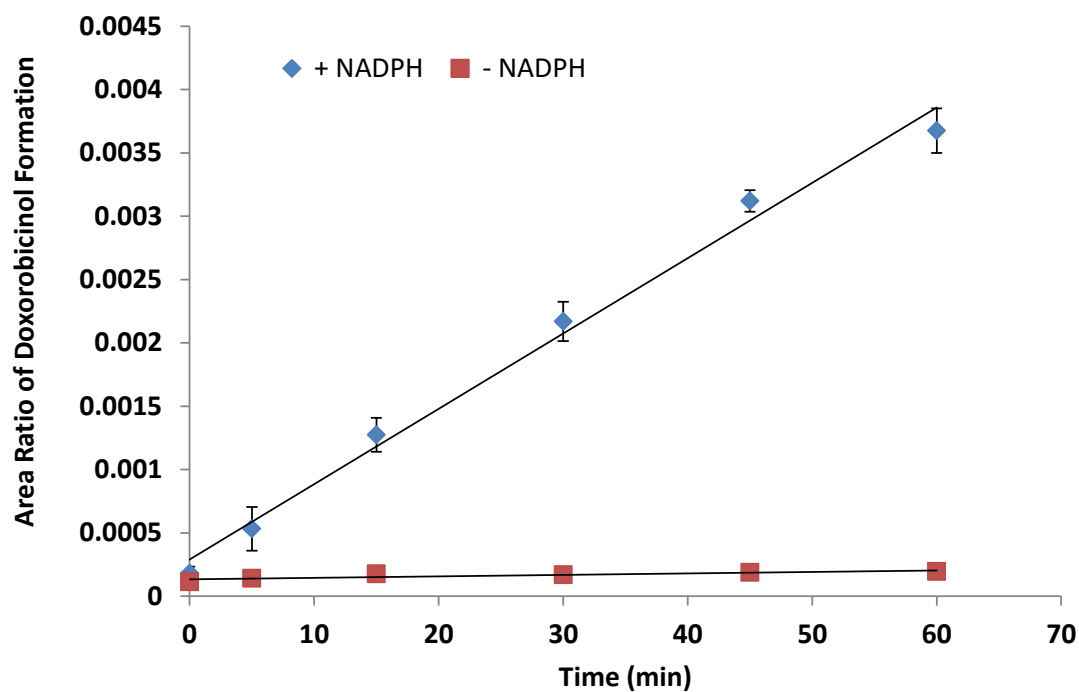
DMD#81083

Figure 3.



DMD#81083

Figure 4.



DMD#81083

Figure 5.

